J. Biochem. **135**, 455–463 (2004)
DOI: 10.1093/jb/mvh059

Purification and Characterization of Recombinant Human Prostacyclin Synthase

Masayuki Wada[1,2], Chieko Yokoyama[*,1], Toshihisa Hatae[1], Manabu Shimonishi[1], Masahiko Nakamura[3], Yoshio Imai[4], Volker Ullrich[5] and Tadashi Tanabe[1,2]

[1]Department of Pharmacology, National Cardiovascular Center Research Institute and [2]Division of Microcirculatory Kinetics, Osaka University Graduate School of Medicine, National Cardiovascular Center, 5-7-1 Fujishiro-dai, Suita, Osaka 565-8565; [3]Division of Physiology, Institute for Protein Research, Osaka University, Yamada-oka, Suita, Osaka 565-0871; [4]Department of Veterinary Science, Osaka Prefecture University, Sakai, Osaka 599-8531; and [5]Department of Biology, University of Konstanz D-78434, Germany

Received December 2, 2003; accepted January 17, 2004

Prostacyclin synthase (PGIS), which catalyzes the conversion of prostaglandin (PG) H_2 to prostacyclin (PGI_2), is a member of the cytochrome P-450 (P450) superfamily, CYP8A1. To study the enzymatic and protein characteristics of human PGIS, the enzyme was overexpressed in *Spodoptera frugiperda* 21 (Sf21) cells using the baculovirus expression system. PGIS was expressed in the microsomes of the infected Sf21 cells after culture in 5 μg/ml hematin-supplemented medium for 72 h. The holoenzyme was isolated from the solubilized microsomal fraction by calcium phosphate gel absorption and purified to homogeneity by DEAE-Sepharose and hydroxyapatite column chromatography. The K_m and V_{max} values of the purified human PGIS for PGH_2 were 30 μM and 15 μmol/min/mg of protein at 24°C, respectively. The optical absorption and EPR spectra of the enzyme revealed the characteristics of a low-spin form of P450 in the oxidized state. The carbon monoxide-reduced difference spectrum, however, exhibited a peak at 418 nm rather than 450 nm. The addition of a PGH_2 analogue, U46619, to the enzyme produced an oxygen-ligand type of the difference spectrum with maximum absorption at 407 nm and minimum absorption at 430 nm. Treatment with another PGH_2 analogue, U44069, produced a peak at 387 nm and a trough at 432 nm in the spectrum (Type I), while treatment with tranylcypromine, a PGIS inhibitor, produced a peak at 434 nm and a trough at 412 nm (Type II). A Cys441His mutant of the enzyme possessed no heme-binding ability or enzyme activity. Thus, we succeeded in obtaining a sufficient amount of the purified recombinant human PGIS from infected insect cells for spectral analyses that has high specific activity and the characteristics of a P450, indicating substrate specificity.

Key words: baculovirus, CO-reduced spectrum, cytochrome P-450, human, overexpression, prostacyclin synthase.

Abbreviations: BHT, butylated hydroxytoluene; CO, carbon monoxide; ECL, enhanced chemiluminescence; P450, cytochrome P-450; PG, prostaglandin; PGIS, prostacyclin synthase; PGI_2, prostacyclin; PMSF, phenylmethylsulfonyl fluoride; PVDF, polyvinylidene fluoride; Sf21 cells, *Spodoptera frugiperda* 21 cells; TBS-T, Tris buffered salt solution with Tween 20; TXS, thromboxane synthase.

Prostacyclin (PGI_2), a potent inhibitor of platelet aggregation and a powerful vasodilator, plays an important physiological role in the cardiovascular system (*1*, *2*). It is an autocrine and paracrine mediator that binds to the specific G protein-coupled receptor, IP receptor, (*3*) and/or to the nuclear receptor, peroxisome proliferator-activated receptor (PPAR) δ (*4–6*). PGI_2 inhibits the growth of vascular smooth muscle cells (*7*, *8*), and is used as a treatment for primary pulmonary hypertension (*9*). PGI_2 is produced from prostaglandin (PG) H_2 by the enzyme prostacyclin synthase (PGIS) [EC 5.3.99.4]. Transfer of the human PGIS gene has been shown to provide useful gene therapy for vascular diseases such as primary pulmonary hypertension (*10*, *11*), and for restenosis after percutaneous transluminal coronary angioplasty (*8*). More recently, we indicated that the cotransfection of human hepatocyte growth factor and the PGIS genes enhances angiogenesis and leads to an improvement in neuropathy (*12*).

PGIS has been purified from the solubilized microsomal fractions of porcine and bovine aortas as a hemoprotein with a molecular mass of 49–52 kDa, and has been characterized as a cytochrome P-450 (P450) (*13–16*). We have previously cloned bovine, human, rat and mouse PGIS cDNAs, and identified PGIS as a member of the P450 superfamily, CYP8A1, by homology analysis of its primary structure (*16–19*). Although most P450s catalyze monooxygenation reactions, PGIS catalyzes the isomerization of PGH_2 to PGI_2 (*20*). A possible mechanism for the enzyme reaction is the recognition of the endoperoxide oxygen at C-11 of PGH_2 by PGIS, followed

*To whom correspondence should be addressed. Tel: +81-6-6833-5012 (ext. 2596), Fax: +81-1-6-6872-8090, E-mail: yokoyama@jsc.ri.ncvc.go.jp

by cleavage of the O-O bond, and the conversion of PGH_2 to PGI_2. In the enzyme reaction, PGIS does not require an electron donor such as NADPH. Site-directed mutagenesis studies of the enzyme using a mammalian cell expression system have demonstrated that the heme-binding cysteine residue and the EXXR motif in helix K, which are well conserved among P450s, are important regions for PGIS activity (*21*, *22*). However, although attempts have been made to develop PGIS-based gene therapies for vascular diseases, as mentioned above, the enzymatic properties of human PGIS remain to be characterized in detail due to the difficulty in obtaining sufficient human material for kinetic and spectral analyses. Large amounts of purified enzyme are also needed for a full protein structural analysis. To overcome this difficulty, we have developed a method whereby intact human PGIS can be produced using the baculovirus expression system. Here, we describe the purification and characterization of human PGIS after overexpression in insect cells using the baculovirus expression system.

EXPERIMENTAL PROCEDURES

Materials—*Spodoptera frugiperda* (Sf21) insect cells, the BAC-to-BAC™ Baculovirus Expression System, Grace's insect medium, yeastolate, lactalbumin hydrolysate, and C_{ELL} FECTIN™ reagent were purchased from Invitrogen. [1-^{14}C]Arachidonic acid (1.85 GBq/mmol) and HiTrap DEAE FF (5 ml) were obtained from Amersham Biosciences, and Macro-Prep Ceramic Hydroxyapatite (Type I, 20 μm) was obtained from Bio-Rad. U44619 and U44069 were purchased from Cayman, tranylcypromine hydrochloride from Sigma, microsomes from sheep vesicular glands from Oxford Biomedical Research, and precoated Silica Gel 60 glass plates for TLC from Merck.

Cell Culture—Sf21 cells were maintained by suspension culture at between 0.5×10^6 and 2.5×10^6 cells/ml in Grace's insect cell culture medium supplemented with 10% fetal bovine serum, 0.4% yeastolate and 0.4% lactalbumin hydrolysate at 27°C.

Expression of Recombinant Human PGIS Using the BAC-to-BAC™ Baculovirus Expression System—Human PGIS cDNA from the pCMV/PGISwt plasmid (*21*) was inserted into the *Sal*I and *Bam*HI sites of the pBluescript II SK+ vector (pBlue/hPGISwt). The cDNA was then subcloned into the pFastBac-1 donor plasmid at the *Sal*I and *Not*I sites. The constructed plasmid (pFast/hPGISwt) was transfected into competent DH10Bac cells. Colonies containing the recombinant bacmid DNA were selected and isolated according to the manufacturer's instructions. To generate the recombinant baculovirus, the recombinant bacmid DNA was transfected into Sf21 cells (1×10^6 cells/35 mm dish) using C_{ELL} FECTIN™ reagent and incubated at 27°C for 72 h. The medium containing the recombinant baculovirus was collected by centrifugation at 500 ×*g* for 10 min and the virus was amplified for further use.

Sf21 cells (2×10^8 cells) were harvested into two 50-ml conical polypropylene tubes, and 10 ml culture medium containing the recombinant baculovirus (1×10^9 pfu) was added to each tube. For infection with the recombinant viruses, the Sf21 cells were incubated at 27°C and gently resuspended every 10 min. After 1 h, the infected cells (2×10^8 cells/20 ml) were transferred to a 500-ml spinner flask containing 180 ml Grace's insect cell culture medium supplemented with 10% fetal bovine serum, 0.4% yeastolate, 0.4% lactalbumin hydrolysate and 5 μg/ml hematin (*23*). The cells were harvested at 72 h after infection by centrifugation at 500 ×*g* for 5 min, and washed once with supplement-free medium. The cell precipitate was stored at –80°C until use.

Expression of Mutated Human PGIS (Cys441His) and Mouse Thromboxane Synthase (TXS) Using the BAC-to-BAC™ Baculovirus Expression System—The cDNA for a mutated form of human PGIS, with a Cys441 to His replacement (*21*), was subcloned into the *Sal*I and *Bam*HI sites of the pBluescript II SK+ vector (pBlue/hPGISCys441His). The hPGISCys441His cDNA and mouse TXS cDNA (*19*) were then subcloned into the pFastBac-1 donor plasmid at the *Sal*I and *Not*I sites. The remaining steps in the expression procedure were carried out as described above.

Purification of Recombinant Human PGIS—All manipulations were carried out at 4°C. The microsomal fractions of the cells were prepared according to the method of Ullrich, *et al* (*24*). The cells harvested from two-spinner flasks (4×10^8 cells) were suspended in 50 ml of 100 mM potassium phosphate buffer, pH 7.5, containing 1 mM EDTA, 0.1 mM DTT, 0.1 mM butylated hydroxytoluene (BHT), 2 μg/ml leupeptin, 2 μg/ml pepstatin and 44 μg/ml phenylmethylsulfonyl fluoride (PMSF), and sonicated four times at level setting 3 for 10 s using an ultrasonicator (ASTRASON, model XL2020). The homogenate was centrifuged at 8,000 ×*g* for 15 min, and the resulting supernatant was further centrifuged at 105,000 ×*g* for 60 min. The precipitate was suspended in 25 ml of 100 mM potassium phosphate buffer, pH 7.5, containing 1 mM EDTA, 0.1 mM DTT, 0.1 mM BHT and 100 mM KCl, using a glass-teflon homogenizer, and then centrifuged at 105,000 ×*g* for 60 min. The precipitate (microsomal fraction) was resuspended in 20 ml of 10 mM potassium phosphate buffer, pH 7.5, containing 20% glycerol, 0.1 mM EDTA, 0.1 mM DTT and 0.1 mM BHT (Buffer A).

A mixture (2.67 ml) of 1.7% (v/v) Lubrol PX and 4.25% (w/v) cholate was added to the microsomal suspension (20 ml) under stirring to give a final concentration of 0.2% Lubrol PX and 0.5% cholate. The suspension was stirred gently for 40 min at 4°C, and then centrifuged at 105,000 ×*g* for 60 min. The supernatant (solubilized enzyme) was applied to 170 mg of calcium phosphate gel (*25*) that had previously been equilibrated with Buffer A and suspended. After centrifugation at 2,000 ×*g* for 5 min, the supernatant was collected. The precipitated gel was washed with 7 ml of 10 mM potassium phosphate buffer, pH 7.5, containing 20% glycerol, 0.1 mM EDTA, 0.2% Lubrol PX and 0.5% cholate. After centrifugation at 2,000 ×*g* for 5 min, the supernatant was collected and mixed with the first supernatant to form the enzyme fraction.

The supernatant was applied to a HiTrap DEAE FF column (5 ml) connected to an ÄKTApurifier (Amersham Biosciences) equilibrated with Buffer A containing 0.1% Lubrol PX. The column was washed with one bed-volume of Buffer A containing 0.05% Lubrol PX and 0.2% cholate, and then with two bed-volumes of 50 mM NaCl; finally, the enzyme was eluted with a linear gradient of 50–200 mM NaCl at a flow rate of 1 ml/min. The protein concen-

tration and the amount of heme binding PGIS (holoenzyme) in the eluate were monitored by measuring the absorption at 280 and 420 nm, respectively.

The fractions (5 ml) containing the PGIS activity were concentrated with Centriprep-30 concentrators (Amicon) and diluted to 5 ml with 10 mM potassium phosphate buffer, pH 7.5, containing 20% glycerol. This manipulation was repeated four times until the conductivity of the concentrated sample reached that of the hydroxyapatite equilibration buffer (Buffer A). The enzyme fraction was finally concentrated to 2 ml.

A hydroxyapatite column (1.6 × 3 cm) connected to an ÄKTApurifier was equilibrated with Buffer A. After applying the sample, the column was washed with Buffer A containing 0.2% Lubrol PX and 0.5% cholate at a flow rate of 0.3 ml/min. The peak fractions exhibiting absorbance at 420 nm were collected and stored at –80°C until required for characterization of the enzyme.

Preparation of an Anti-mouse PGIS Antibody—For the expression of murine PGIS fused with an N-terminal polyhistidine (6xHis) tag, mouse PGIS cDNA (*19*) was inserted into pRSET C (Invitrogen) for high-level prokaryotic expression, and the coding region of the fusion protein was cloned into pFastBac-1. The histidine-tagged mouse PGIS fusion protein was expressed in Sf21 cells using the BAC-to-BAC™ baculovirus expression system and purified by Ni^{2+}-chelating Sepharose column chromatography. After SDS-PAGE the band containing the mouse PGIS protein was excised from the gel. About 100 μg of the purified protein was mixed with complete Freund's adjuvant and injected into Japanese white rabbits. These animals received three further booster doses at 2-week intervals. The rabbit serum cross-reacted with human PGIS and was used as a PGIS antibody.

SDS-PAGE and Immunoblotting Analysis—Proteins were separated by 10% SDS-PAGE according to the method of Laemmli, and the protein bands were detected by silver staining (silver stain II kit, Wako, Osaka). For immunoblotting analysis, the proteins were transferred electrophoretically onto a polyvinylidene fluoride (PVDF) membrane (Millipore) for 1.5 h at 1.5 mA/cm^2. The membrane was blocked with 5% skim milk in 20 mM Tris-HCl, pH 7.5, containing 500 mM NaCl and 0.05% Tween 20 (Tris-buffered salt solution with Tween 20, TBS-T) at room temperature overnight. Subsequently, the membrane was blocked with 1% BSA in TBS-T at room temperature for 1 h, then incubated with the rabbit serum containing the polyclonal antibody against mouse PGIS for 1 h. After the membrane had been rinsed three times with TBS-T for 10 min each time, it was incubated with horseradish peroxidase-conjugated anti-rabbit IgG (Daco) in TBS-T containing 1% BSA for 1 h. After four further 10-min washes with TBS-T, the membrane was allowed to react with enhanced chemiluminescence (ECL) detection reagents (Amersham Biosciences), and exposed to X-ray film. The protein concentration was determined using the BCA protein assay reagent kit (Pierce). The molecular weight of the protein was calibrated using Rainbow colored protein molecular weight markers (Amersham Biosciences).

Amino Acid Sequence of the N-terminus of Recombinant Human PGIS—The purified enzyme (540 μg) was diluted into 100 μl of 0.1% trifluoroacetic acid (TFA) and applied to the PVDF membrane of a ProSorb™ sample preparation cartridge (Applied Biosystems) equilibrated with methanol. The membrane was washed twice with 0.1% TFA and methanol, and then dried. The dried PVDF membrane was put onto the cartridge of the protein sequencer (Procise cLC491, Applied Biosystems), and the amino acid sequence was analyzed.

Enzyme Assays—For the conventional assay (assay A), the reaction mixture (100 μl) contained 0.1 M Tris-HCl buffer, pH 7.4, [1-^{14}C]arachidonic acid (80,000 cpm/5 nmol/5 μl of ethanol), 250 μg of microsomes from sheep vascular glands, and the enzyme preparations. For the determination of PGIS activity (assay B), the reaction mixture (100 μl) contained 0.1 M Tris-HCl, pH 7.4, [1-^{14}C]PGH_2 (80,000 cpm/0.3–5 nmol/5 μl acetone) and the enzyme preparations. [1-^{14}C]PGH_2 was prepared from [1-^{14}C]arachidonic acid using microsomes from sheep vesicular glands as described previously (*16*). In both cases, the reaction was started by the addition of substrate and was carried out at 24°C for a specified time. The reaction was terminated by adding 300 μl of a mixture of ethylether/methanol/0.2 M citric acid (30:4:1) that had been precooled to –20°C. The organic phase (100 μl) was applied directly to a TLC plate at 4°C. The TLC plate was developed at 24°C with an organic solvent composed of ethyl acetate/2,2,4-trimethylpentane/acetic acid/water (110:50:20:100). The radioactivity on the TLC plate was measured using a Fujix Bio-image analyzer BAS 2500 (Fuji Photo Film, Tokyo).

Optical Spectroscopy—Optical spectra were recorded using a Jasco V-550 UV/VIS spectrophotometer. For the measurement of the carbon monoxide (CO) difference spectra in the reduced state, the purified sample (200 μl) was flushed with N_2 gas to purge it of O_2, next with CO gas for 1 min, and then the sample was reduced by the addition of 1.5 μl of sodium dithionite solution (300 mg/ml) (*26*). Optical difference spectra after the addition of the PGH_2 analogues U46619 and U44069, and the PGIS inhibitor of tranylcypromine hydrochloride were measured between 350 nm and 500 nm (*13*, *27*).

EPR Spectroscopy—Five milliliters of the enzyme-containing fraction from DEAE chromatography was concentrated to 250 μl by centrifugation at 105,000 ×*g* for 60 h at 4°C. The concentrated enzyme was subjected to EPR spectroscopic analysis. EPR spectra were recorded at a microwave frequency of 9.5 GHz (X-band) on a Bruker ESP300E spectrometer with a dual mode resonator and peripheral equipment as described (*28*).

RESULTS

Expression of Recombinant Human PGIS—Human PGIS was expressed in Sf21 cells using the Bac-to-Bac baculovirus expression system. It has been reported that the addition of exogenous heme to the culture medium increases the enzyme activity of P450s expressed using the baculovirus system (*29*). When the transfected Sf21 cells were cultured with various concentrations of hematin, the PGIS activity in the microsomal fractions increased dose-dependently up to 5 μg/ml hematin, but decreased when the hematin concentration exceeded 5 μg/ml. On the other hand, no PGIS activity was detected when the infected cells were cultured without hematin.

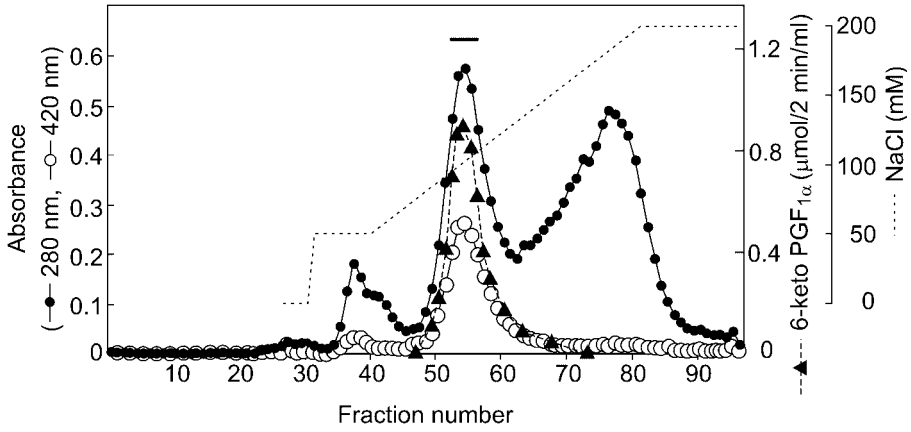

Fig. 1. **Purification of human PGIS by DEAE-Sepharose column chromatography.** The calcium phosphate gel-treated microsomal fraction of Sf21 cells was applied to a HiTrap DEAE FF column as described under "EXPERIMENTAL PROCEDURES," and 1-ml fractions were collected. The NaCl concentration increased as shown by the broken line. The protein and hemoprotein concentrations were monitored by absorption at 280 nm (closed circles) and 420 nm (open circles), respectively. The enzymatic activity (open triangles) was measured using a conventional enzymatic activity assay (assay A) as described under "Experimental Procedures". Pooled fractions are indicated by the bar.

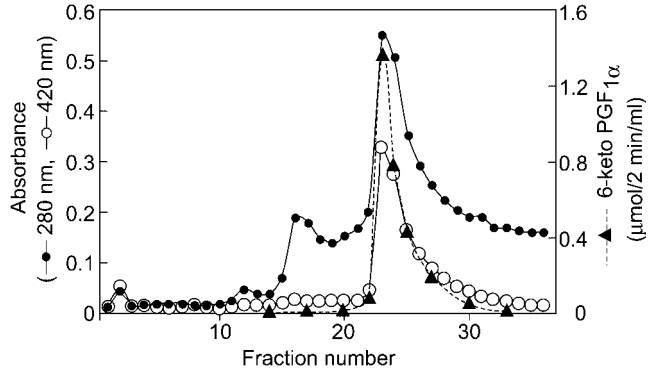

Fig. 2. **Purification of human PGIS by hydroxyapatite column chromatography.** The concentrated, partially purified enzyme obtained by DEAE-Sepharose column chromatography was loaded onto a hydroxyapatite column as described under "EXPERIMENTAL PROCEDURES." Protein and hemoprotein concentrations and enzyme activity were monitored as described in the legend to Fig. 1.

Although the enzyme activity in the cultured cells increased time-dependently up to 96 h in the presence of hematin, cell viability decreased after 72 h. Thus, the infected cells were cultured for 72 h in medium containing 5 μg/ml hematin.

Purification of Recombinant Human PGIS—When the solubilized Sf21 microsomes were subjected to chromatography on a DEAE-Sepharose column eluted with approximately 100 mM NaCl, an enzyme activity peak consistent with an absorption peak appeared at 420 nm. However, fairly large amounts of recombinant protein were detected by SDS-PAGE and immunoblot analysis in fractions eluting later. These fractions contained the PGIS protein with a low absorption at 420 nm and exhibited little enzyme activity, indicating the possibility of an apoenzyme. Calcium phosphate gel was used to remove the inactive form from the solubilized microsomal fractions. Most of the inactive form was trapped in the calcium phosphate gel and the highly active holoenzyme was recovered in the supernatant. As shown in Fig. 1, the application of the calcium phosphate gel-treated solubilized microsomal fraction to the DEAE-Sepharose column resulted in a single peak of enzymatic activity, associated with an absorbance peak at 420 nm, that appeared between 80 and 100 mM NaCl. The active fractions (5 ml) were pooled and concentrated to 2 ml. The concentrated enzyme was applied to a hydroxyapatite column, and the enzyme was eluted as described in "EXPERIMENTAL PROCEDURES." The resulting enzymatic activity peak was consistent with the peaks for both protein and absorbance at 420 nm (Fig. 2). The specific activity of the final preparation was about 7 μmol/min/mg protein (Table 1).

Figure 3 shows the results of SDS-PAGE and immunoblot analysis at each step in the purification of human PGIS. The purified enzyme yielded an apparently single band on SDS-PAGE, and reacted with the PGIS polyclonal antibody. Although the molecular weight of human PGIS is 57,103 (calculated on the basis of the primary structure deduced from the cDNA sequence) (*17*), the purified enzyme migrated as a band of about 48 kDa as compared with the molecular weight markers. We, therefore, determined the N-terminal amino acid sequence of the purified enzyme to investigate whether the enzyme was truncated. The resulting sequence of 20 N-terminal amino acids (NH_2-Met-Ala-Trp-$(Ala)_2$-$(Leu)_2$-Glu-$(Leu)_2$-$(Ala)_2$-$(Leu)_7$-Ser-) was completely identical to that of the human PGIS. Furthermore, an antibody raised against the synthetic C-terminal peptide corresponding to amino acid residues 485–500, P4 (*6*), also recognized the purified enzyme (data not shown). These results indicate that the purified recombinant enzyme has intact N-terminal and C-terminal regions, and that it migrates on SDS-

Table 1. **Purification of expressed recombinant human PGIS from Sf21 cells.**

Purification step	Protein (mg)	Specific activity (μmol/min/ mg)	Total activity (μmol/min)	Yield (%)
Homogenate	500	–	–	–
Solubilized microsomes	25.5	1.6	39.8	100
Calcium phosphate gel	16.8	2.6	43.7	109.7
DEAE-Sepharose chromatography	1.5	4.3	6.5	16.3
Hydroxyapatite chromatography	0.2	7.1	1.4	3.5

Assay B was used to measure enzyme activity; the reaction was stopped at 5 s.

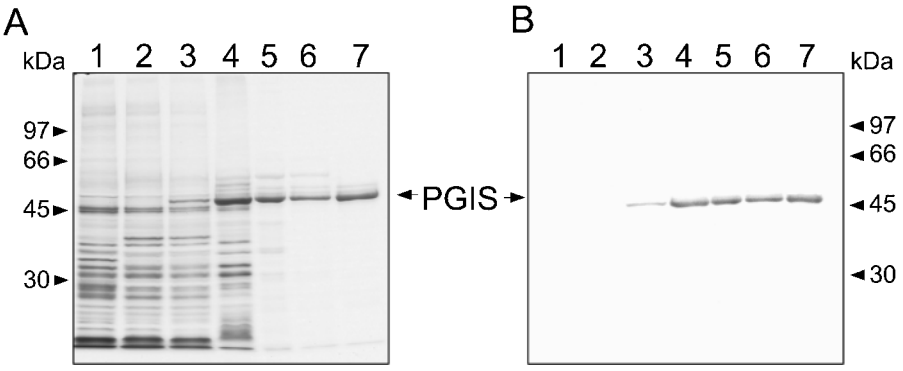

Fig. 3. **SDS-PAGE of human PGIS at various purification steps.** (A) Silver staining. (B) Immunoblot analysis. Lane 1, cell homogenate (15 μg of protein); Lane 2, mock-infected cell homogenate (15 μg of protein); Lane 3, cell homogenate infected with a recombinant PGIS-carrying virus (15 μg of protein); Lane 4, solubilized Sf21 cells microsomes (9 μg of protein); Lane 5, calcium phosphate gel supernatant (3 μg of protein); Lane 6, HiTrap DEAE FF column elute (2 μg of protein); Lane 7, hydroxyapatite column elute (1 μg of protein).

PAGE with a smaller apparent molecular weight than the calculated value.

Activity of Purified Human PGIS—Figure 4A shows the time courses for the production of 6-keto-$PGF_{1\alpha}$, a stable degradation product of the conversion of PGH_2 to PGI_2, with various amounts of the purified enzyme. Although the reaction proceeded in an almost linear fashion until 5 s at 24°C, the reaction process slowed thereafter. The conversion of PGH_2 to 6-keto-$PGF_{1\alpha}$ increased at a rate proportional to the amount of purified enzyme present for enzyme concentrations of up to 1 μg (Fig. 4B). The K_m and V_{max} values for purified human PGIS at 24°C, calculated from the Lineweaver-Burk plot, are about 30 μM and about 15 μmol/min/mg protein, respectively (Fig. 4C).

Spectral Properties of Human PGIS in the Oxidized State—Figure 5A shows the optical absorption spectra obtained with purified human PGIS. The oxidized enzyme (Fig. 5A, solid line) produced a maximal peak in the Soret band at 420 nm, and peaks at 570 nm and 538 nm in the α and β bands, respectively; this is an absorption spectrum for the mainly low-spin type of P450 in the ferric state. A small peak at 630 nm in the charge transfer band and the small shoulder visible at 392 nm might indicate the presence of a small amount of the high-spin form. To confirm that the heme iron of human PGIS is in the oxidized state, EPR spectroscopic analysis was carried out using the DEAE-Sepharose eluate fraction of the enzyme. In the oxidized state, the EPR-spectrum was consistent with the low-spin tensor of oxidized P450-enzymes, showing g-values at 2.463, 2.262 and 1.957 (Fig. 6) (*30*). This confirms that the human PGIS is a low-spin type of P450.

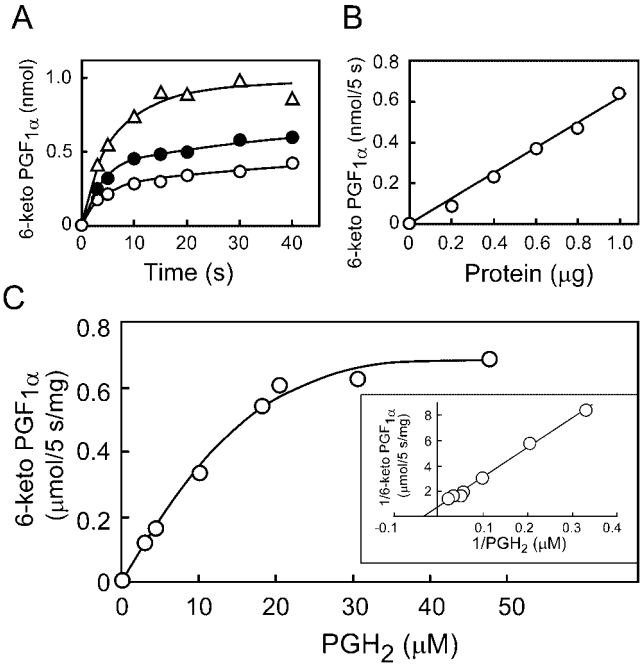

Fig. 4. **Enzymatic properties of purified human PGIS.** Enzyme activity was measured using assay B, as described under "EXPERIMENTAL PROCEDURES." (A) Time course of the human PGIS reaction at enzyme concentrations of 0.2 μg (open circles), 0.54 μg (closed circles), and 0.8 μg (open triangles). The dependency on the amount of enzyme present (B) and the substrate-saturation curve for human PGIS (C) are also shown. The enzyme reaction was allowed to proceed for 5 s. The inset shows the Lineweaver-Burk plot.

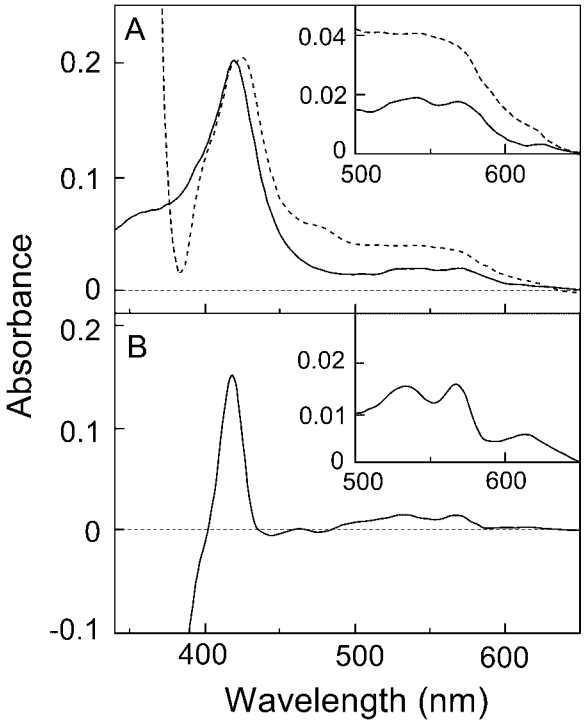

Fig. 5. **Spectral properties of human PGIS.** The purified enzyme (145 μg/ml) was dissolved in 100 mM potassium phosphate buffer, pH 7.5, containing 20% glycerol, 0.1 mM EDTA, 0.2% Lubrol PX and 0.5% cholate and used for analysis. A, spectrum of the oxidized enzyme (—), and spectrum of the reduced enzyme (- - -); B, CO-reduced difference spectrum.

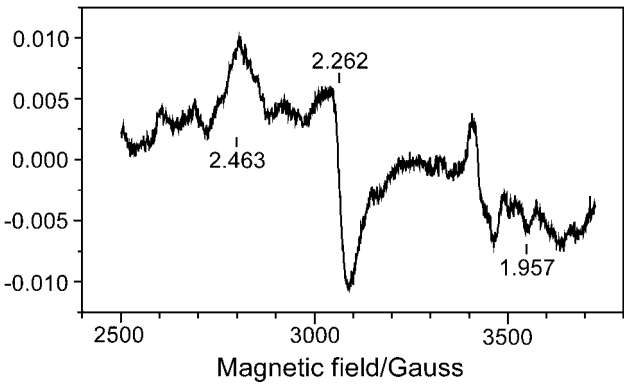

Fig. 6. **EPR spectrum of human PGIS.** The peak enzyme fractions from DEAE-Sepharose column chromatography were concentrated by ultracentrifugation, and the concentrated sample (8.3 mg/ml) was subjected to EPR spectral analysis as described in "EXPERIMENTAL PROCEDURES."

The Reduction Spectrum and the CO-Reduced Difference Spectrum—After reduction of the enzyme with sodium dithionite, the spectrum shows a sharp peak at 424 nm and a broad peak at 548–564 nm (Fig. 5A, broken line). The CO-reduced difference spectrum for human PGIS shows a peak at 418 nm rather than at 450 nm, although the spectrum was continuously monitored from immediately after the reaction start of the CO-reduction up to 40 minutes (Fig. 5B). Furthermore, no peak at 450 nm was observed when the crude enzyme fraction was analyzed after treatment with CO and sodium dithionate. In contrast, the CO-reduced difference spectra of the purified P450 from rabbit liver and solubilized microsomes from both Sf21 cells overexpressing mouse TXS and phenobarbital-treated mouse liver showed a peak at around 450 nm during control experiments (data not shown). In other words, the CO-reduction spectral analysis technique worked well with other P450s expressed in our baculovirus-insect cell system and in mouse liver. Therefore, the human PGIS might be significantly unstable in the reduction and/or reduction-CO binding states.

Substrate Difference Spectra—Since substrate analogue-enzyme and inhibitor-enzyme binding difference spectral data were available for bovine PGIS (*27*, *31*), the purified human PGIS was subjected to the same spectral analyses so that its characteristics could be compared with those of the bovine enzyme. U46619 is a stable PGH_2 analogue in which the endoperoxide oxygen at C-9 is replaced by an ethyl group. The difference spectrum of human PGIS treated with U46619 showed a maximum at 407 nm and a minimum at 430 nm, typical of oxygen ligand binding to heme iron in the ferric state (Fig. 7A). In contrast, when the enzyme was treated with another stable PGH_2 analogue, U44069, in which the endoperoxide oxygen at C-11 of PGH_2 is replaced by an ethyl group, the difference spectrum showed a maximum at 387 nm and a minimum at 432 nm, which can be classified as a Type I spectrum reflecting the binding of a substrate (Fig. 7B) (*32*). The difference spectrum after treatment with a PGIS inhibitor, tranylcypromine, exhibited a maximum at 434 nm and a minimum at 412 nm, which can be classified as a Type II spectrum reflecting the interaction of inhibitors with the enzyme (Fig. 7C) (*13*). These spectra conform to

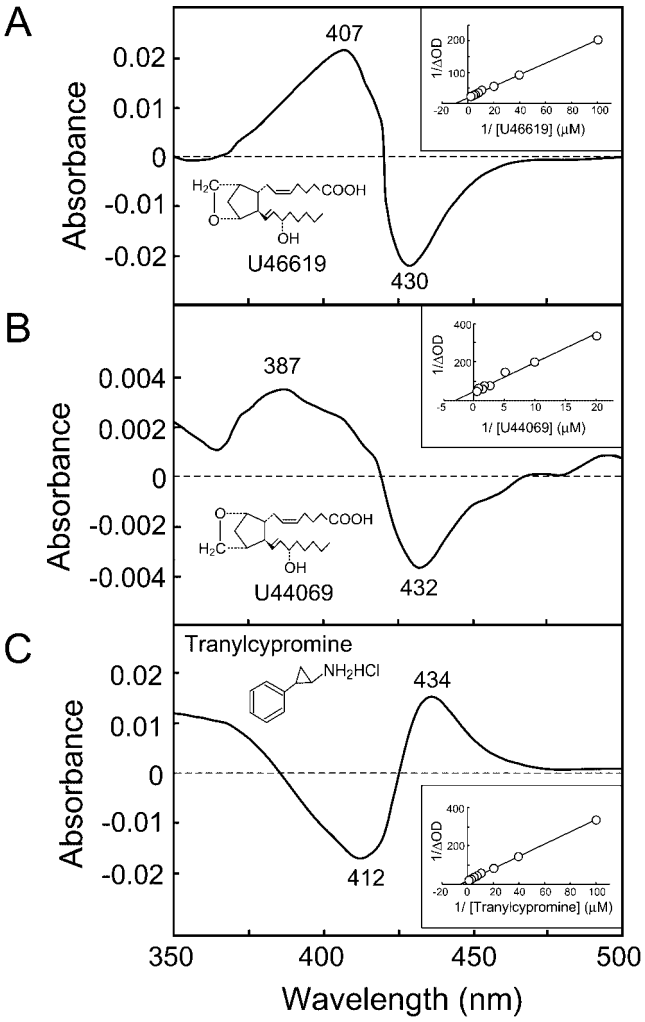

Fig. 7. **Optical difference spectra and concentration-dependence of the human PGIS reaction with the PGH_2 analogues U44619 and U44069, and the PGIS inhibitor tranylcypromine.** Purified human PGIS (162 μg/ml, dissolved in 100 mM potassium phosphate buffer, pH 7.5, containing 20% glycerol, 0.1 mM EDTA, 0.2% Lubrol PX, and 0.5% cholate) was incubated with (A) U46619 (10–1000 μM, dissolved in ethanol), (B) U44069 (50–1,200 μM, dissolved in ethanol) or (C) tranylcypromine-HCl (10–1,400 μM dissolved in water). The figures show the difference spectra for the enzyme treated with each compound at a concentration of 400 μM. The inserts show the Lineweaver-Burk plots of the maximum and minimum values for the difference absorption spectra.

those of the bovine enzyme. The apparent spectral dissociation constants of U46619, U44069 and tranylcypromine, calculated from the Lineweaver-Burk plot, were 110, 308 and 224 μM, respectively (Fig. 7 insets). These results strongly suggest that the purified recombinant human PGIS has an intact substrate binding site near the distal side of the heme and recognizes the endoperoxide oxygen at C-11 of the substrate specifically.

Cys441 of the Proximal Heme Ligand—To confirm the role of Cys441 as the fifth ligand of heme in human PGIS, the Cys441His mutant PGIS was expressed in Sf21 cells under the same conditions as those used for the wild-type enzyme. The Cys441His mutant migrated as a band of about 48 kDa on SDS-PAGE and was recognized by the

anti-PGIS antibody. However, the mutant had no enzymatic activity and did not show any significant absorbance from heme at around 420 nm. Thus, it was confirmed that Cys441 is essential for heme binding, and that heme is essential for the enzyme reaction.

DISCUSSION

We succeeded in purifying a sufficient amount of recombinant human PGIS to characterize its enzymatic properties. This was done without structural modifications, such as a histidine tag, using a baculovirus-insect cell expression system. Approximately 200 μg of the active enzyme containing heme was obtained from 4×10^8 cells, and the specific activity of the purified enzyme was 7 μmol/min/mg protein, which is 3.5-fold that of the PGIS purified from bovine aorta (*16*). The K_m of our purified human PGIS was 30 μM, which is also about 3 times higher than that previously reported for bovine PGIS (*15*, *16*). The activity of the enzyme did not increase linearly, and the reaction slowed within 5 s even if excess substrate was present in the reaction mixture. This observation supports the idea that PGIS is a "suicide enzyme" as previously reported (*33*). According to the results of the spectral studies, the purified recombinant human PGIS appears to be a low spin P450 based on the optical absorption and EPR spectra recorded in the oxidized state. Furthermore, the results of the difference spectra for substrate analogues and inhibitor of PGIS show features of P450 and indicate the substrate specificity of the enzyme.

The distal side of the heme is important as the substrate binding pocket, and most P450s contain a conserved threonine residue in helix I that works as a site of proton transfer and an important residue for substrate specificity (*34*). However, although PGIS shows the typical substrate difference spectrum of oxygen ligand binding to heme iron in the ferric state with the substrate analogue, U46619, the Thr is not conserved in helix I of PGIS. While sterol 12α-hydroxyrase (CYP8B1), which is a monooxygenase and shows the highest homology with PGIS, retains a threonine residue in the region corresponding to the O_2-binding pocket. In human PGIS, the amino acid residue corresponding to the conserved Thr is speculated to be Met288 by the alignment of sequences (*35*). These findings suggest that a conserved Thr at the distal heme surface is not essential for the PGIS reaction because it is not a redox reaction, and the Thr may not be important for recognizing the endoperoxide oxygen at C-11 of PGH_2.

The absorbance peak of the human PGIS did not shift to around 450 nm upon reduction by dithionate in the presence of CO, although we subjected a high concentration of purified enzyme with a high specific activity to optical absorption spectral analysis. Previously the PGIS purified from porcine aortic microsomes by affinity chromatography with U46619, has been reported to yield an absorption maximum at 417 nm in the Soret band under oxidized conditions, and a peak at 451 nm arises after adding CO to the reduced PGIS (*14*). The reduced enzyme, however, was converted time-dependently to a cytochrome P420-like hemoprotein with a maximal absorption at 421 nm. With bovine PGIS, the CO-reduced absorption spectrum exhibited peaks at 440 nm (*15*) or 451 nm (*16*) after purification of the enzyme by immunoaffinity chromatography or by conventional methods; however, chemical reduction by sodium dithionate in the presence of CO is slow and incomplete (*36*). These results suggest that PGIS is unstable in the reduced state. Especially, human PGIS might be denatured a few seconds before or after forming a CO-complex in its reduced state, and the peak band appearing at 420 nm reflects the inactive form of a P450. It has been reported that the CO reduced spectrum of mutant P450 2C2 that results from the substitution of Thr301 with Lys in helix I is rapidly converted to the denatured form (*37*). In contrast, TXS (CYP5A1), which interacts with the endoperoxide oxygen at C-9 of PGH_2 and catalyzes the isomerization of PGH_2 to TXA_2, shows a maximum peak at 450 nm in its CO-reduced state (*38*, *39*), although the Thr is not conserved in the enzyme; Ile346 of human TXS corresponds to the conserved Thr in helix I (*40*). Thus, differences in the amino acid residue on the distal heme suface might be involved in the stability of the enzyme in the reduced state. Furthermore, considering that the primary structure of PGIS shares only 16% identity with that of TXS, and that TXS has a long insertion between helix H and helix I, differences in the structure(s) around the oxygen-binding region may affect the binding of reduced human PGIS to CO. Additionally, the sequence of the proximal heme-binding domain of human PGIS is WGAGHNHCLG (434–443), and the Phe and Arg/His of the conserved FXXGXR/HXCXG residues of P450s are replaced by Trp and Asn, respectively, in this enzyme. In contrast, the heme-binding domain of TXS is completely conserved. The catalytic activity of a mutant PGIS, in which Ala replaces Asn439, was slightly higher than that of wild-type PGIS (*22*), while the mutation of Arg478 to Ala in the heme-binding domain of TXS reduced the level of expressed protein and abolished enzyme activity (*40*). It has also been reported that the substitution of Arg454 with Leu in rat liver $P450_d$ reduces catalytic activity to 80% of that seen with the wild type enzyme, and that the Soret peak appearing at 448 nm in the CO-reduced difference spectrum of the mutant is unstable, disappearing quickly while a peak at 420 nm appears (*41*). Thus, structural differences on the proximal side of the heme also might be involved in enzyme stability. From these structural differences surrounding the heme and the fact that O_2 is not involved in the PGIS reaction, it seems to be a peculiar characteristic of human PGIS that the absorbance of the enzyme does not shift to 450nm under in CO-reduced conditions.

The cysteine residue of the proximal ligand of heme is conserved in PGIS and other P450s. Tomura *et al.* reported that, after substitution of histidine for cysteine, the fifth axial ligand for heme in *Fusarium oxysporum* $P450_{nor}$ retains a weak but significant level of enzyme activity (*42*). This observation suggests that histidine may be able to function as a heme ligand in $P450_{nor}$ such as myoglobin. Previously, we expressed a Cys441His-mutant form of human PGIS in HEK 293 cells in order to examine the role of Cys441 in human PGIS, and found that this mutant possesses no detectable enzyme activity as measured by a conventional enzyme assay (*21*). However, it remains unclear whether the mutant enzyme pro-

tein can bind to a heme prosthetic group. The Cys441His mutant expressed in Sf21 cells under the same conditions as those used for the wild-type enzyme show no significant enzymatic activity or absorbance near 420 nm. These observations indicate that heme is an essential prosthetic group for the enzyme reaction, and that the substitution of His for Cys441 in the enzyme leads to a loss of the heme-binding function. Therefore, Cys441 is probably important for the incorporation and/or retention of heme by PGIS.

In this study, we succeeded in the purification and characterization of the recombinant human enzyme of a normal and natural type of PGIS. The purified PGIS exhibited high activity and specific characteristics of P450. PGIS is probably too unstable under reduced conditions to allow any distinction of catalytic reaction and structural differences in the environments around the heme group and helix I region between PGIS and other P450s. It is hoped that large-scale expression of human PGIS will become possible using the baculovirus expression system and a scale-up of our purification system, and that this will be helpful for crystal structure analysis as well as for analyses of the mechanisms involved in the reactions of human PGIS.

We thank Dr. P.M. Kroneck (University of Konstanz) for obtaining the EPR spectra, Drs. J. Tanaka and N. Minamino (National Cardiovascular Center Research Institute) for performing the amino acid sequence analysis, and Y. Ogawa, T. Sugimoto, S. Bandoh and M. Miyazaki for their technical assistance. This work was supported in part by grants from the Ministry of Health, Labour and Welfare of Japan; Grants-in-Aid for Scientific Research from the Ministry of Education, Culture, Sports, Science, and Technology of Japan; and the Promotion of Fundamental Studies in Health Science of the Organization for Pharmaceutical Safety and Research (OPSR) of Japan.

REFERENCES

1. Moncada, S., Gryglewski, R., Bunting, S., and Vane, J.R. (1976) An enzyme isolated from arteries transforms prostaglandin endoperoxides to an unstable substance that inhibits platelet aggregation. *Nature* **263**, 663–665
2. Moncada, S. and Vane, J.R. (1978) Pharmacology and endogenous roles of prostaglandin endoperoxides, thromboxane A2, and prostacyclin. *Pharmacol. Rev.* **30**, 293–331
3. Negishi, M., Sugimoto, Y., and Ichikawa, A. (1995) Molecular mechanisms of diverse actions of prostanoid receptors. *Biochim. Biophys. Acta* **1259**, 109–119
4. Forman, B.M., Chen, J., and Evans, R.M. (1997) Hypolipidemic drugs, polyunsaturated fatty acids, and eicosanoids are ligands for peroxisome proliferator-activated receptors alpha and delta. *Proc. Natl Acad. Sci. USA* **94**, 4312–4317
5. Gupta, R.A., Tan, J., Krause, W.F., Geraci, M.W., Willson, T.M., Dey, S.K., and DuBois, R.N. (2000) Prostacyclin-mediated activation of peroxisome proliferator-activated receptor delta in colorectal cancer. *Proc. Natl. Acad. Sci. USA* **97**, 13275–13280
6. Hatae, T., Wada, M., Yokoyama, C., Shimonishi, M., and Tanabe, T. (2001) Prostacyclin-dependent apoptosis mediated by PPAR δ. *J. Biol. Chem.* **276**, 46260–46267
7. Hara, S., Morishita, R., Tone, Y., Yokoyama, C., Inoue, H., Kaneda, Y., Ogihara, T., and Tanabe, T. (1995) Overexpression of prostacyclin synthase inhibits growth of vascular smooth muscle cells. *Biochem. Biophys. Res. Commun.* **216**, 862–867
8. Todaka, T., Yokoyama, C., Yanamoto, H., Hashimoto, N., Nagata, I., Tsukahara, T., Hara, S., Hatae, T., Morishita, R., Aoki, M., Ogihara, T., Kaneda, Y., and Tanabe, T. (1999) Gene transfer of human prostacyclin synthase prevents neointimal formation after carotid balloon injury in rats. *Stroke* **30**, 419–426
9. McLaughlin, V.V., Genthner, D.E., Panella, M.M., and Rich, S. (1998) Reduction in pulmonary vascular resistance with long-term epoprostenol (prostacyclin) therapy in primary pulmonary hypertension. *N. Engl. J. Med.* **338**, 273–277
10. Geraci, M., Gao, B., Shepherd, D., Allard, J., Curiel, D., Westcott, J., and Voelkel, N. (1998) Pulmonary prostacyclin synthase overexpression by adenovirus transfection and in transgenic mice. *Chest* **114**, 99S
11. Nagaya, N., Yokoyama, C., Kyotani, S., Shimonishi, M., Morishita, R., Uematsu, M., Nishikimi, T., Nakanishi, N., Ogihara, T., Yamagishi, M., Miyatake, K., Kaneda, Y., and Tanabe, T. (2000) Gene transfer of human prostacyclin synthase ameliorates monocrotaline-induced pulmonary hypertension in rats. *Circulation* **102**, 2005–2010
12. Koike, H., Morishita, R., Iguchi, S., Aoki, M., Matsumoto, K., Nakamura, T., Yokoyama, C., Tanabe, T., Ogihara, T., and Kaneda, Y. (2003) Enhanced angiogenesis and improvement of neuropathy by cotransfection of human hepatocyte growth factor and prostacyclin synthase gene. *FASEB J.* **6**, 779–781
13. Ullrich, V., Castle, L., and Weber, P. (1981) Spectral evidence for the cytochrome P450 nature of prostacyclin synthetase. *Biochem. Pharmacol.* **30**, 2033–2036
14. Graf, H. and Ullrich, V. (1982) Prostacyclin synthase as a cytochrome P450 enzyme. in *Cytochrome-P450, Biochemistry, Biophysics and Environmental Implication* (Hietanen, E., Laitinen, M., and Hanninen, O., eds) pp. 103–106, Elsevier Biomedical Press, B.V.
15. DeWitt, D.L. and Smith, W.L. (1983) Purification of prostacyclin synthase from bovine aorta by immunoaffinity chromatography. Evidence that the enzyme is a hemoprotein. *J. Biol. Chem.* **258**, 3285–3293
16. Hara, S., Miyata, A., Yokoyama, C., Inoue, H., Brugger, R., Lottspeich, F., Ullrich, V., and Tanabe, T. (1994) Isolation and molecular cloning of prostacyclin synthase from bovine endothelial cells. *J. Biol. Chem.* **269**, 19897–19903
17. Miyata, A., Hara, S., Yokoyama, C., Inoue, H., Ullrich, V., and Tanabe, T. (1994) Molecular cloning and expression of human prostacyclin synthase. *Biochem. Biophys. Res. Commun.* **200**, 1728–1734
18. Tone, Y., Inoue, H., Hara, S., Yokoyama, C., Hatae, T., Oida, H., Narumiya, S., Shigemoto, R., Yukawa, S., and Tanabe, T. (1997) The regional distribution and cellular localization of mRNA encoding rat prostacyclin synthase. *Eur. J. Cell Biol.* **72**, 268–277
19. Kuwamoto, S., Inoue, H., Tone, Y., Izumi, Y., and Tanabe, T. (1997) Inverse gene expression of prostacyclin and thromboxane synthases in resident and activated peritoneal macrophages. *FEBS Lett.* **409**, 242–246
20. Ullrich, V. and Brugger, R. (1994) Prostacyclin and thromboxane synthase: new aspect of hemethiolate catalysis. *Angew. Chem. Int. Ed. Engl.* **33**, 1911–1919
21. Hatae, T., Hara, S., Yokoyama, C., Yabuki, T., Inoue, H., Ullrich, V., and Tanabe, T. (1996) Site-directed mutagenesis of human prostacyclin synthase: Alteration of Cys441 of the Cys-pocket, and Glu347 and Arg350 of the EXXR motif. *FEBS Lett.* **389**, 268–272
22. Shyue, S.K., Ruan, K.H., Wang, L.H., and Wu, K.K. (1997) Prostacyclin synthase active sites. Identification by molecular modeling-guided site-directed mutagenesis. *J. Biol. Chem.* **272**, 3657–3662
23. Ohta, D., Matsu-ura, Y., and Sato, R. (1991) Expression and characterization of a rabbit liver cytochrome P450 belonging to P450IIB subfamily with the aid of the baculovirus expression vector system. *Biochem. Biophys. Res. Commun.* **175**, 394–399
24. Ullrich, V., Brugger, R., Lottspeich, F., and Siegle, I. (1997) Properties of prostacyclin synthase. *Adv. Exp. Med. Biol.* **400A**, 113–119

25. Heppel, L.A. (1955) Inorganic pyrophosphatase from yeast. *Methods Enzymol.* **2**, 570–577
26. Omura, T. and Sato, R. (1967) The carbon monoxide-binding pigment of liver microsomes. II. Solubilization, purification and properties. *J. Biol. Chem.* **239**, 2379–2385
27. Ullrich, V. and Hecker, M. (1990) A concept for the mechanism of prostacyclin and thromboxane A_2 biosynthesis. *Adv. Prostaglandin Thromboxane Leukot. Res.* **20**, 95–101
28. Neese, F., Zumft, W.G., Antholine, W.E., and Kroneck, P.M.H. (1996) The purple mixed-valence CuA center in nitrous-oxide reductase: EPR of the copper-63-, copper-65-, and both copper-65- and [^{15}N]histidine-enriched enzyme and a molecular orbital interpretation. *J. Amer. Chem. Soc.* **118**, 8692–8699
29. Asseffa, A., Smith, S.J., Nagata, K., Gillette, J., Gelboin, H.V., and Gonzalez, F.J. (1989) Novel exogenous heme-dependent expression of mammalian cytochrome P450 using baculovirus. *Arch. Biochem. Biophys.* **274**, 481–490
30. Graf, H., Ruf, H.-H., and Ullrich, V. (1983) Prostacyclin synthase, a cythochrom P450 enzyme. *Angew. Chem. Int. Ed. Engl.* **22**, 487–488
31. Hecker, M. and Ullrich, V. (1989) On the mechanism of prostacyclin and thromboxane A_2 biosynthesis. *J. Biol. Chem.* **264**, 141–150
32. Yoshida, Y. and Kumaoka, H. (1975) Studies on the substrate-induced spectral change of cytochrome P-450 in liver microsomes. *J. Biochem. (Tokyo)* **78**, 55–68
33. Watanabe, K., Yamamoto, S., and Hayaishi, O. (1979) Reactions of prostaglandin endoperoxides with prostaglandin I synthetase solubilized from rabbit aorta microsomes. *Biochem. Biophys. Res. Commun.* **87**, 192–199
34. Fukuda, T., Imai, Y., Komori, M., Nakamura, M., Kusunose, E., Satouchi, K., and Kusunose, M. (1994) Different mechanisms of regioselection of fatty acid hydroxylation by laurate (omega-1)-hydroxylating P450s, P450 2C2 and P450 2E1. *J. Biochem. (Tokyo)* **115**, 338–3445
35. Eggertsen, G., Olin, M., Andersson, U., Ishida, H., Kubota, S., Hellman, U., Okuda, K.I., and Bjorkhem, I. (1996) Molecular cloning and expression of rabbit sterol 12α-hydroxylase. *J. Biol. Chem.* **271**, 32269–32275
36. Tanabe, T. and Ullrich, V. (1995) Prostacyclin and thromboxane synthases. *J. Lipid Mediat. Cell Signal.* **12**, 243–255
37. Imai, Y. and Nakamura, M. (1991) Nitrogenous ligation at the sixth coordination position of the Thr-301 to Lys-mutated P450IIC2 heme iron. *J. Biochem. (Tokyo)* **110**, 884–888
38. Haurand, M. and Ullrich, V. (1985) Isolation and characterization of thromboxane synthase from human platelets as a cytochrome P-450 enzyme. *J. Biol. Chem.* **260**, 15059–15067
39. Hsu, P.Y., Tsai, A.L., Kulmacz, R.J., and Wang, L.H. (1999) Expression, purification, and spectroscopic characterization of human thromboxane synthase. *J. Biol. Chem.* **274**, 762–769
40. Wang, L.H., Matijevic-Aleksic, N., Hsu, P.Y., Ruan, K.H., Wu, K.K., and Kulmacz, R.J. (1996) Identification of thromboxane A_2 synthase active site residues by molecular modeling-guided site-directed mutagenesis. *J. Biol. Chem.* **271**, 19970–19975
41. Shimizu, T., Hirano, K., Takahashi, M., Hatano, M., and Fujii-Kuriyama, Y. (1988) Site-directed mutageneses of rat liver cytochrome P-450$_d$: axial ligand and heme incorporation. *Biochemistry* **27**, 4138–4141
42. Tomura, D., Sai, G., Endo, M., Kudo, T., and Shoun, H. (1995) Analysis of cytochrome P-450nor by protein engineering technology (in Japanese). *Seikagaku* **67**, 592